EurJOC European Journal of Organic Chemistry

FULL PAPER

DOI: 10.1002/ejoc.201500170

The Dynamic Assembly of Covalent Organic Polygons: Finding the Optimal Balance of Solubility, Functionality, and Stability

Merry K. Smith,[a] Alexander R. Goldberg,[a] and Brian H. Northrop*[a]

Keywords: Self-assembly / Macrocycles / Borates

Six variably functionalized phenanthrene-based bis(catechol) derivatives have been synthesized and their ability to undergo dynamic covalent assembly with 1,4-benzenediboronic acid (**BDBA**) to give discrete, shape-persistent [2+2] assemblies has been investigated. Systematically varying the functionality of the bis(catechol) derivatives is found to influence both the reaction conditions necessary to promote their self-assembly with **BDBA** as well as the stability of the resulting assemblies in the presence of protic solvents. A model is proposed to describe how solvent choice and starting material functionality must be carefully balanced in order to shift many competing equilibria toward the formation of discrete, soluble covalent organic polygons. The results are expected to provide additional insight into optimizing the synthesis of other boronate ester polygons/polyhedra as well as related, "infinite" covalent organic frameworks (COFs).

Introduction

The thermodynamically driven dynamic assembly[1] of extended framework materials has been the focus of increasing interest in the materials science community over the past two decades with the emergence of metal organic frameworks[2] (MOFs) in the mid-1990s[3] and the discovery of covalent organic frameworks[4] (COFs) in 2005.[5] Formed through the reversible covalent linkage of organic subunits, COFs are particularly attractive synthetic targets, in large part because of their many advantageous physical properties. These lightweight, highly ordered, porous polymers exhibit high thermal stabilities, low densities, tunable pore sizes and high internal surface areas,[4a–4c,5,6] leading to potential applications in optoelectronics,[7] electron transport,[8] heterogeneous catalysis,[9] and gas sequestration and storage.[10] According to the principles of reticular chemistry[11] coupled with the selection of appropriately reversible dynamic covalent reactions, specific combinations of organic subunits can allow for the rational design of COFs with predictable framework geometries, pore sizes, and chemical properties. Boronic acids have proven especially useful in this regard as they are able to reversibly self-condense into boroxine anhydrides and can also undergo dynamic assembly with diols, such as catechol derivatives, to produce boronate esters.[12] Both systems are well suited for the modular assembly of periodic 2- and 3-dimentional COFs; indeed, structurally diverse polyfunctional boronic acids and oligo-catechols have been used to produce the majority of COFs to date.[4a–4c,13]

Despite the increasing interest in the synthesis and characterization of COFs derived from boronic acids, discrete assemblies formed from boronic acids are less common. Examples of porous covalent organic polygons or polyhedra (COPs) prepared from boronic acid and oligo-catechol monomers include porous boronate-ester cages, macrocycles, capsules, and cavitands, and boroxine cyclophanes.[14–19] Related examples of discrete boronic acid based assemblies have also been reported as complexes with sp^2 hybridized nitrogen compounds.[12,20] Generally absent from this array of macromolecules are discrete assemblies that are structurally analogous to COFs and prepared from monomers that are similar or identical to those used to prepare extended frameworks. If soluble, these "COF analogue" COPs can aid in elucidating the dynamic and kinetic details of COF formation and may provide insight regarding the optimization of solvent systems and reaction conditions used in COF synthesis. Furthermore, discrete COPs are porous, shape-persistent[21] structures with potential applications that may extend beyond those of COFs, as they are likely to form aggregates and higher-order assemblies in solution and on solid substrates. With their potential to form higher-order assemblies in solution, COPs may find applications as liquid crystalline materials,[22,23] in self-assembled monolayer formation,[24] and in solution-processable organic photovoltaics.[7c,7d] Additionally, soluble boronate ester assemblies offer opportunities to tune their solid-state suprastructures[25] through coordination[20] with Lewis basic groups such as bipyridyls.

In spite of their potential, there remain very few examples of discrete, shape-persistent assemblies derived from boronic acids, likely because their synthesis and study is

[a] Department of Chemistry, Wesleyan University,
52 Lawn Avenue, Middletown, CT 06459, USA
E-mail: bnorthrop@wesleyan.edu
http://www.bnorthrop.faculty.wesleyan.edu

Supporting information for this article is available on the WWW under http://dx.doi.org/10.1002/ejoc.201500170.

complicated by the same difficulties that have made the characterization and study of COF materials quite challenging. In particular, the inherent insolubility of boronic acid derived COFs, most COPs, and their boronic acid secondary building units (SBUs) has presented several challenges to their preparation and characterization. In the roughly twenty years since the first reports of MOFs, over 6,000 distinct MOF structures[2c] have been synthesized and characterized. In a dramatic contrast, over the nine years since the first report of a COF fewer than 50 distinct COFs have been reported in the literature.[4b] Similarly, in contrast to the many examples of single crystalline MOFs, no single crystal of a boronic acid derived COF has been reported. To date, and to the best of our knowledge, only four examples of single crystalline COFs have been reported in the literature.[26,27] The insolublity of COFs has also been a significant barrier to detailed mechanistic and kinetic analysis of COF formation, however Dichtel and co-workers have recently demonstrated that turbidity analysis can be used to quantify the kinetics of early stage COF formation from within homogeneous reaction solutions,[28] a considerable advance in the study of COFs and related materials. Still, the insolubility of such frameworks remains a persistent challenge to their characterization, investigation, and synthetic optimization.

Those groups that have reported soluble, discrete assemblies based on boronic acid (Scheme 1) have been forced to confront issues related to poor solubility. Kobayashi and co-workers reported[16] soluble boronate ester cavitands based on tetra-boronic acid calixarenes and 1,2-bis(3,4-dihydroxyphenyl)ethane. Despite the inherent flexibility of both the calixarene and the bis(catechol) starting materials, tetra-functionalization of the calixarene with alkyl groups (heptyl or phenylethyl) was necessary to promote assembly formation and to ensure the solubility of the resulting cages. In the related realm of boroxine anhydrides, the triply ferrocene-bridged boroxine cyclophane reported by Miljanić and co-workers[19] could be obtained upon crystallization out of a solution of mesitylene and dioxane (1:1), but was otherwise poorly soluble. In a previous work, we reported[29] the synthesis and characterization of soluble covalent organic boronate ester rectangles composed of rigid triphenyl bis(catechol) derivatives and benzenediboronic acid. Hexyloxy functionalization was found to be necessary for solution phase self-assembly and characterization. Very recently, Mastalerz and co-workers synthesized[18a] an impressive mesoporous cuboctahedral boronate ester cage by refluxing a tetrahydroxy triptycene derivative and 1,3,5-benzene triboronic acid in chloroform. The introduction of solubilizing ethyl-groups on the triptycene monomer was found to be essential for cage assembly and analysis. The solubility of the boronate ester cuboctahedron was found to be so precarious that, upon desolvation, the resulting solid could not be redissolved to any extent. Collectively, these results highlight the sensitivity of dynamic covalent assembly to the solubility of both the secondary building unit (SBU) precursors and the desired assemblies themselves.

The preparation of assemblies derived from boronic acid is further complicated by their often-observed sensitivity to the choice of reaction solvent or solvents. The choice of an appropriate solvent system that promotes the high-yielding formation of desired assemblies from within complex, dy-

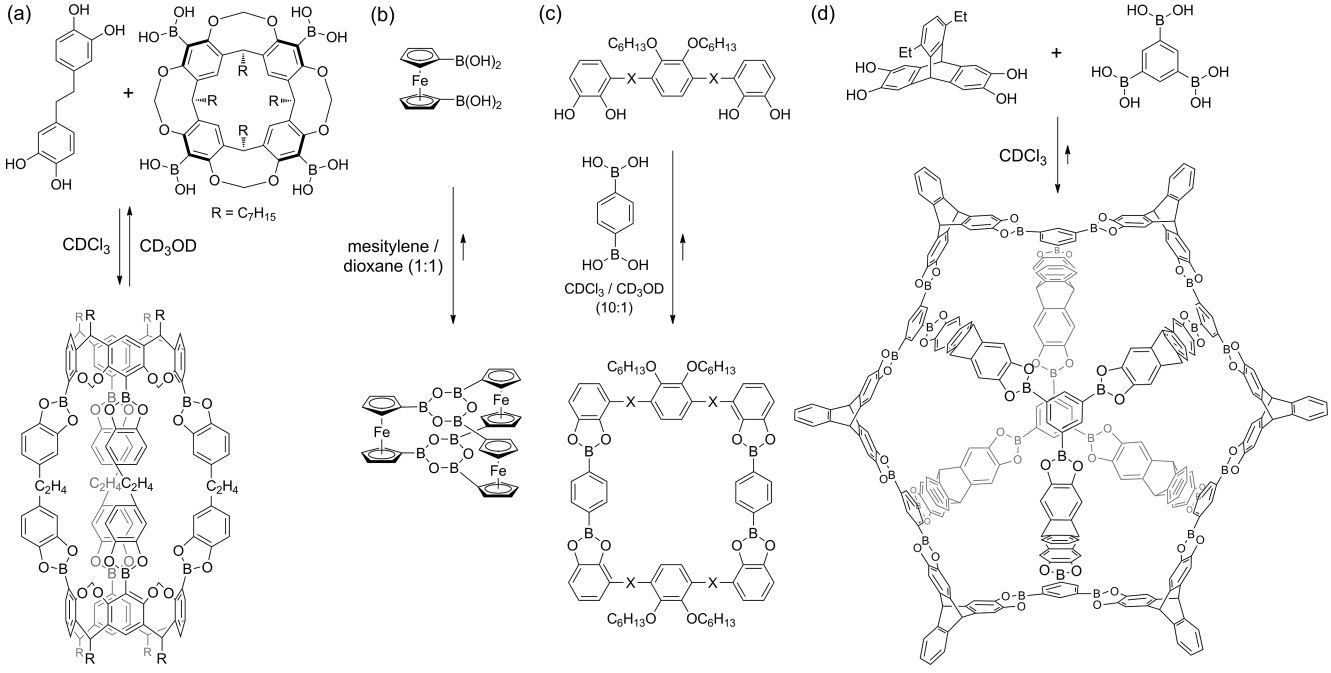

Scheme 1. Representative examples of discrete, shape-persistent assemblies that incorporate boronic acid secondary building units (SBUs): (a) calixerene-based assemblies investigated by Kobayashi,[16] (b) a ferrocene-bridged boroxine cyclophane reported by Miljanić,[19] (c) boronate ester rectangles,[29] and (d) triptycene-based boronate ester cuboctahedra reported by Mastalerz.[18a]

namically exchanging mixtures of oligomers and secondary building units often requires combinatorial screening of many different solvent mixtures in varying ratios. There is considerable literature precedent[15a,16a,16d,17b,17c,18,29] for the dynamic assembly of boronate ester materials in hydrophobic solvents such as dichloromethane, chloroform, toluene, and benzene. Boronate ester COFs, by contrast, are typically synthesized under solvothermal conditions in mixtures of mesitylene and dioxane.[4–7] Some examples of discrete assemblies derived from boronic acid have also been prepared in mesitylene:dioxane (1:1), such as the ferrocene-based boroxine cyclophane prepared by Miljanić and co-workers[19] (Scheme 1, b). With respect to the other discrete, shape-persistent boronate ester assemblies presented in Scheme 1, the mesoporous cubeoctahedron prepared by Mastalerz and co-workers (Scheme 1, d) was assembled in chloroform.[18a] Chloroform has also been used by Kobayashi and co-workers[16] (Scheme 1, a) to prepare boronate ester cavitands. Protic solvents such as methanol, ethanol, and water have played varying roles in the synthesis of boronate ester and boroxine anhydride assemblies. The formation of boronate ester rectangles (Scheme 1, c), for example, could not be achieved in pure chloroform,[29] however a mixture of chloroform and methanol (10:1) gave the desired rectangles in high yields. Dichtel[28] and Lavigne[13a,13d] have demonstrated that the addition of small amounts of methanol or water can increase the rate of boronate ester assembly and COF formation in solution, while Wan[24e] and Lackinger[24d,24f] have observed similar phenomena during the formation of COFs on solid substrates. It is believed that these small quantities of protic solvents likely catalyze the dynamic exchange of boronic acid and catechol derivatives. Iwasawa has even observed[17c] that the molar ratio and concentration of mixtures involving benzene, chloroform, and methanol can select for different diastereomeric boronate ester macrocycles from within complex mixtures. Large equivalents of methanol or water, however, have been shown by Kobayashi,[16a] Lavigne,[30] and us[29] to promote the disassembly of boronate ester assemblies and frameworks. To complicate matters further, the ferrocene-based boroxine anhydride assembly shown in Scheme 1 (b) can be soaked in pure ethanol without any disruption of the assembly,[19] however the assembly hydrolyzes within minutes in the presence of water.

From these examples alone it is clear that the successful formation of assemblies based on boronic acid, whether infinite (COFs) or discrete (COPs), is significantly influenced by both SBU structure and the choice of solvent(s). A careful balance must be struck between providing (i) sufficient solubility of the starting material SBUs to initiate assembly, (ii) adequate reversibility of initial oligomers and kinetic intermediates to allow for error correction, and (iii) a robust tolerance of thermodynamically stable product assemblies within the solvent mixture such that they do not revert back to starting materials. Ultimately, the structures and solubilities of both starting materials and products in a given sol-

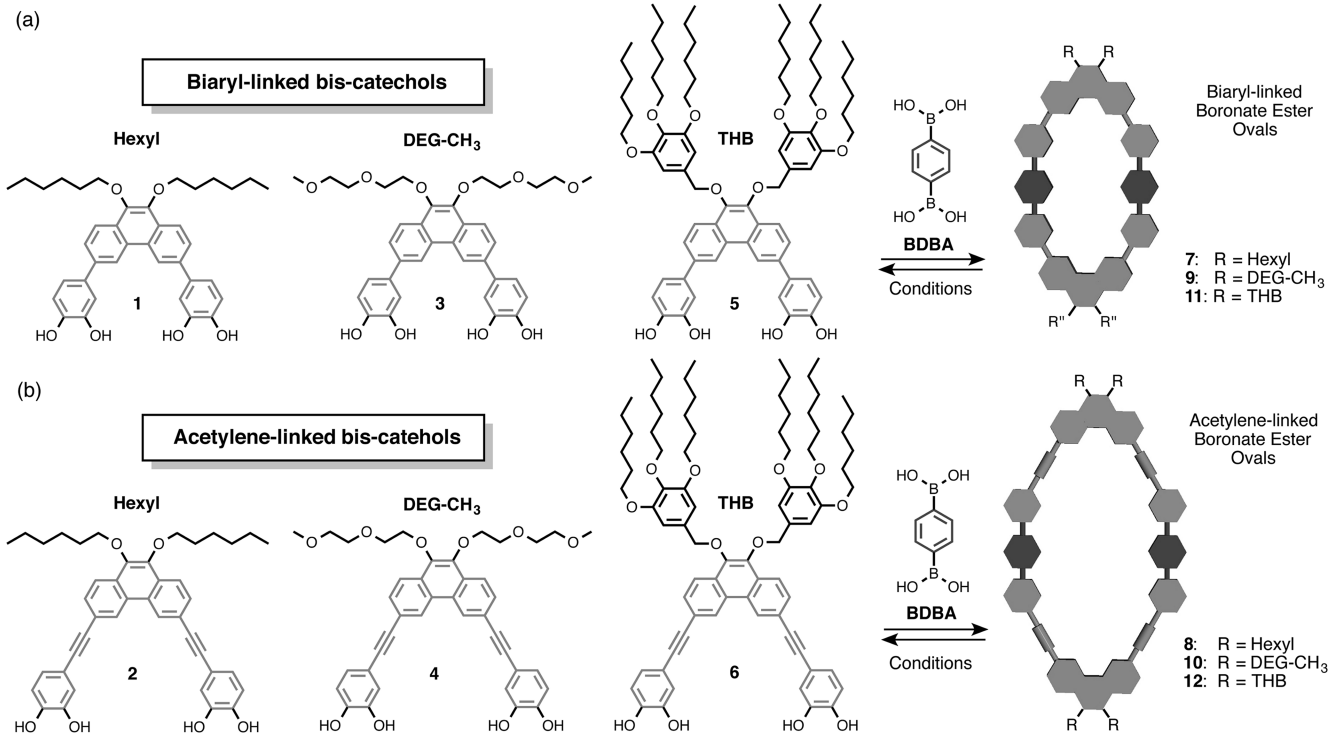

Figure 1. Chemical structures of phenanthrene-based bis(catechol) derivatives **1**–**6** functionalized with hexyloxy (hexyl), diethylene glycol monomethyl ether (DEG-CH_3), or 1,3,5-tris(hexyloxy) benzyl (THB) groups to vary their solution phase characteristics. Biaryl-linked bis(catechol) derivatives are shown in (a) while π-extended, acetylene-linked bis(catechol) derivatives are shown in (b). The bis(catechol)s are designed to self-assembly with 1,4-benzenediboronic acid (**BDBA**) to give shape-persistent boronate ester ovals **7**–**12**.

vent mixture will determine both what species are present at equilibrium, how stable they are, and what analytical methods can be used to investigate them.

Herein we expand upon earlier work in the area of soluble boronate ester rectangles to explore, in greater depth, the roles that starting material and product solubilities play in the synthesis and analysis of discrete boronate ester assemblies. In the current study, we report the synthesis of six variably functionalized, phenanthrene-based bis(catechol) derivatives and evidence for their dynamic self-assembly with benzene-1,4-diboronic acid (**BDBA**) to form shape-persistent boronate ester ovals (Figure 1). Insight gained from examining the influence of different solubilizing groups attached to the phenanthrene bis(catechol)s will contribute more generally to our overall understanding of assembly formation and help pave the way toward a greater variety of discrete, soluble boronate ester assemblies.

Results and Discussion

In previous investigations of discrete boronate ester rectangles (Scheme 1, c), solubility of linear bis(catechol)s was imparted by functionalization of their central phenyl rings with hexyloxy chains. Upon the successful use of these linear bis(catechol) SBUs in the self-assembly of discrete boronate ester rectangles it became of interest to explore the scope of this synthetic approach. Phenanthrene-based subunits were chosen for the current study in part because of the increased π-conjugation of their polycyclic aromatic core. Boronate ester rectangle assemblies were found to fluoresce in the violet-blue region of the visible spectrum (350–460 nm), and the increased conjugation of phenanthrene may enable fluorescence to be shifted further toward longer wavelengths. Furthermore, multiple routes are available for the addition of solubilizing groups at positions 9 and 10 of phenanthrene as well as subsequent functionalization of positions 3 and 6 with catechol derivatives (Scheme 2). Three different functionalities were added at positions 9 and 10 in an effort to vary the solubility of both the starting bis(catechol) phenanthrene derivatives and their resulting assemblies: hexyloxy substituents (compounds **1** and **2**); diethylene glycol monomethyl ether substituents (DEG-CH_3, compounds **3** and **4**); and 3,4,5-tri(hexyloxy)-benzyl substituents (THB, compounds **5** and **6**). This selection of substituents was chosen to compare the relatively hydrophobic nature of hexyloxy substituents vs. the more hydrophilic nature of DEG-CH_3 substituents, along with the influence of a significantly larger solubilizing group (THB) that has the potential to promote aggregation[31] in solution. The catechol moieties were introduced such that they can be oriented *syn*-periplanar and thus the bis(catechol)s can function as 180° secondary building units. Additionally, the catechol units at positions 3 and 6 of phenanthrene were either linked directly as biaryls (compounds **1**, **3**, and **5**) or linked via an acetylene spacer (compounds **2**, **4**, and **6**). The acetylene-linked compounds (**2**, **4**, **6**, and **24**–**26**) were notably less soluble than their biaryl counterparts, both complicating their purification and resulting in lower product yields. Preparing bis(catechol)s with the two different linkages was valuable as they result in boronate ester assemblies with larger or smaller shape-persistent cores, thus allowing the relationship between increased or de-

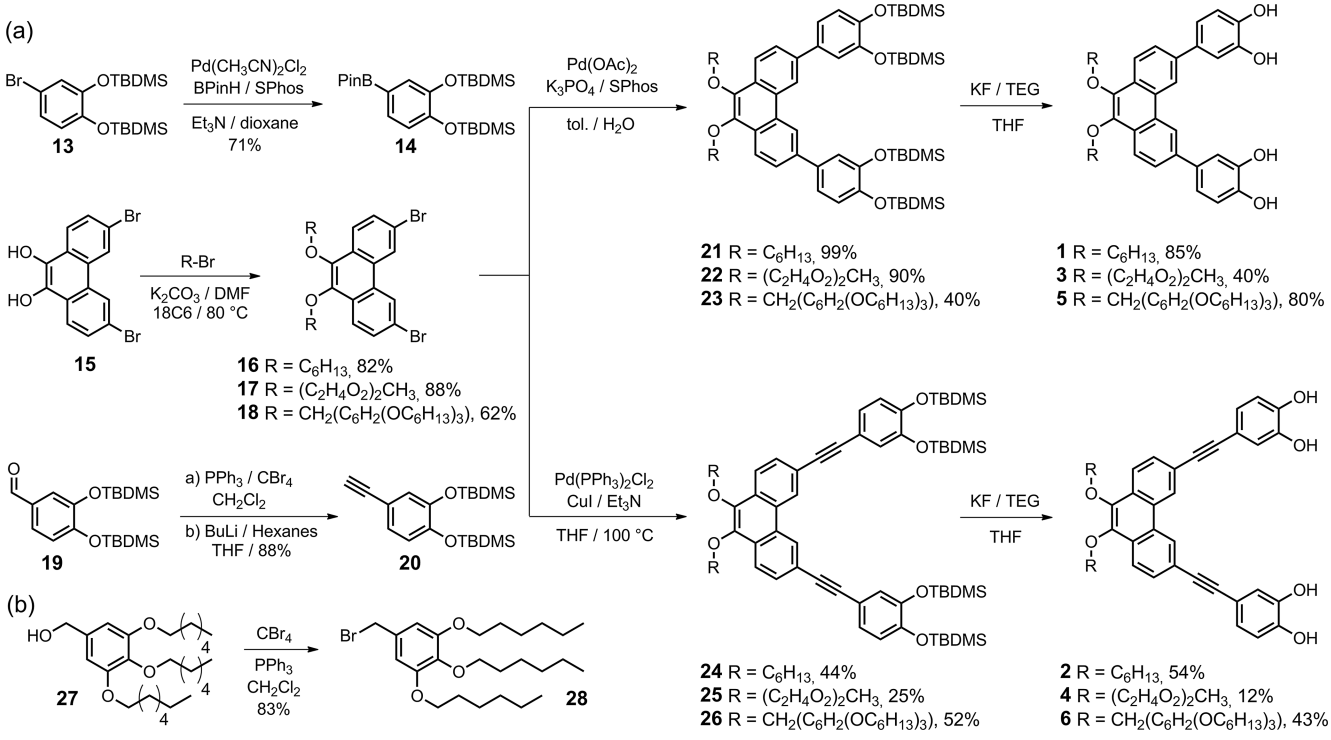

Scheme 2. Synthetic routes to (a) biaryl- and acetylene-linked bis(catechol)s **1**–**6** and (b) 1,3,5-tris(hexyloxy) benzyl derivative **28**.

creased π-surface area and the solubility of resulting assemblies to be investigated. Overall the design is expected to promote the [2+2] condensation of bis(catechol)s **1**–**6** with **BDBA** (Figure 1) to give discrete, oval-shaped boronate ester assemblies.

Sparingly Soluble Assemblies

Initial investigations focused on hexyloxy-functionalized bis(catechol)s **1** and **2**. Both phenanthrene-based bis(catechol) derivatives were found to be poorly soluble in chloroform, despite the presence of two hexyloxy substituents. The di-boronic acid linker **BDBA** is insoluble in chloroform. Combining equimolar amounts of **BDBA** with either **1** or **2** in chloroform leads to heterogeneous mixtures, with no evidence of assembly formation at ambient temperature or upon heating to 50 °C. The addition of 10% methanol, however, aided in the dissolution of both starting materials and promoted their dynamic assembly (Scheme 3).

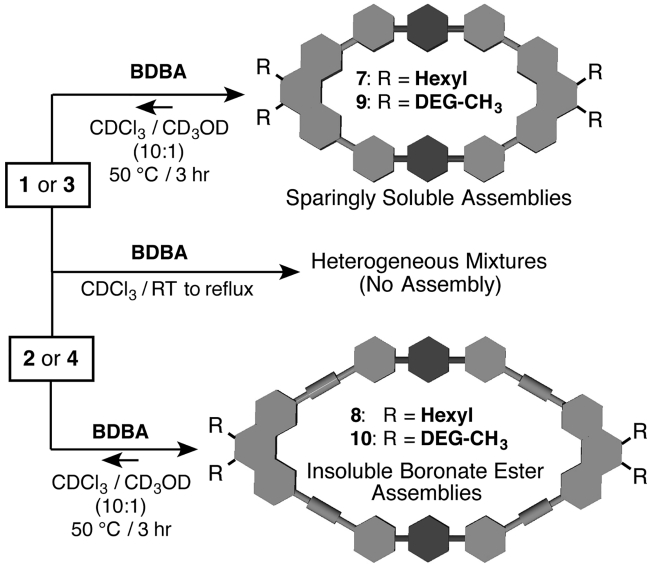

Scheme 3. Assembly of biaryl-linked bis(catechol)s **1** and **3** with **BDBA** in $CDCl_3/CD_3OD$ (10:1) gives sparingly soluble discrete assemblies **7** and **9**. Assembly of acetylene-linked bis(catechol)s **2** and **4** with **BDBA** under the same conditions gives insoluble boronate ester assemblies. Assembly in $CDCl_3$ results in heterogeneous mixtures and no boronate ester formation.

The formation of boronate ester assemblies was evaluated by ^{1}H NMR spectroscopy (CD_3COCD_3). Preliminary evidence supportive of the dynamic assembly of hexyloxy-substituted bis(catechol) **1** and **BDBA** to give boronate ester species was observed by the disappearance of catechol –OH signals at δ = 8.08 and 8.04 ppm along with the appearance of a new singlet at δ = 7.84 ppm corresponding to the incorporation of **BDBA** (see Supporting Information). The overall symmetry of signals observed by ^{1}H NMR spectroscopy suggested the formation of symmetric assemblies, likely corresponding to boronate ester oval **7**. While promising, the low solubility of the assembly prevented conclusive analysis based on ^{1}H NMR spectra alone. Combining acetylene-conjugated bis(catechol) **2** with **BDBA** in $CDCl_3/CD_3OD$ (10:1) and heating to 50 °C resulted in the formation of an insoluble precipitate that precluded analysis by ^{1}H NMR spectroscopy. Attempts to obtain NMR spectra in alternative solvents (C_6D_6, CD_3CN, CD_2Cl_2, CD_3SOCD_3, and $C_2D_2Cl_4$) gave similar results.

The assembly of DEG-CH_3-substituted biaryl- and acetylene-linked bis(catechol)s **3** and **4**, respectively, with **BDBA** under the same conditions gave similar results as related bis(catechol)s **1** and **2**. Stirring and heating an equimolar mixture of **BDBA** with biaryl-linked bis(catechol) **3** resulted in the formation of a sparingly soluble assembly. Analysis by ^{1}H NMR spectroscopy (CD_3COCD_3) again revealed the disappearance of catechol –OH signals between 8.0–8.1 ppm and the concomitant appearance of a singlet at δ = 7.83 ppm consistent with the formation of boronate ester species. The assembly product formed upon mixing **BDBA** with acetylene-linked bis(catechol) **4**, on the other hand, was again found to be insoluble in all available solvents.

NMR spectroscopic analysis consistent with the formation of discrete, shape-persistent boronate ester assemblies **7** and **9** cannot rule out the potential formation of highly symmetric boronate-ester oligomers. Furthermore, NMR analysis of assemblies **8** and **10** provided no insight into their structure as they were insoluble in all available NMR solvents. Accurate mass MALDI mass spectrometry was therefore employed to more conclusively establish the molecularity of assemblies **7**–**10**. The MALDI mass spectra of ovals **7** and **9** reveals peaks of m/z = 1376.6329 $[M]^+$ and 1448.5331 $[M]^+$ respectively (Figure 2). Both these values are in agreement with the calculated values of 1376.6330 for boronate ester assembly **7** and 1448.5297 for boronate ester assembly **9**, quantitatively supporting the formation of the

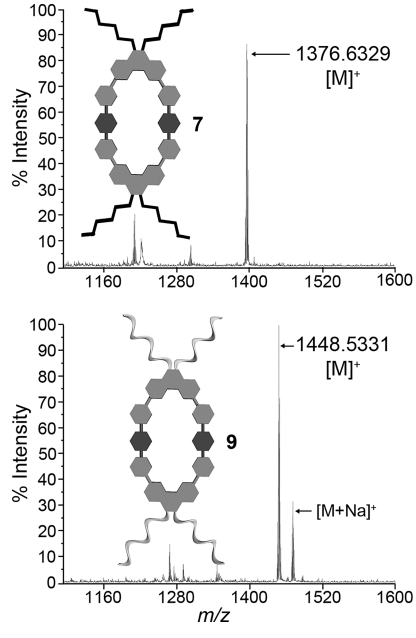

Figure 2. Accurate mass MALDI mass spectra of **7** and **9** reveals that both species are discrete [2+2] boronate ester ovals.

discrete boronate ester ovals. It is interesting to note that the MALDI-MS of **9** reveals a second, weaker signal at m/z = 1471.5298 corresponding to the $[M + Na]^+$ species, potentially resulting from chelation of Na^+ by the DEG-CH_3 substituents of **7**. Quantitative mass spectra of acetylene-conjugated boronate ester assemblies **8** and **10** could not be obtained, likely due to their insolubility.

Infrared (IR) spectroscopy provided more definitive analysis of the chemical structures of boronate ester assemblies **7**–**10**. All four phenanthrene-based bis(catechol) derivatives displayed broad peaks centered at 3300 cm^{-1} corresponding catechol O–H stretching modes. These peaks disappear upon assembly with **BDBA**, indicating the absence of OH functionalities in the resulting assemblies and, by extension, the complete consumption of both bis(catechol) and **BDBA** starting materials. Evidence specific to boronate ester formation is observed primarily in the fingerprint region of the IR spectra of assemblies **7**–**10**. Strong bands centered between 658–660 cm^{-1} were observed for each of the four assemblies, corresponding to out-of-plane displacements of boron and oxygen atoms specific[32] to boronate ester functionalities. Boroxine anhydrides, by contrast, are characterized by out-of-plane boron displacements above 700 cm^{-1}. Furthermore, assemblies **7**–**10** each displayed sharp B–O and C–O stretching modes between 1050–1070 cm^{-1} and between 1230–1250 cm^{-1}, respectively. Stretches in these ranges are also diagnostic of boronate ester functionalities. Overall, IR spectroscopic analysis of assemblies **7**–**10** is supportive of the conclusion that all starting materials have been consumed (absence of O–H stretching modes) and boronate esters have been formed. No evidence of the formation of boroxine anhydride species could be found, indicating consumption of **BDBA** occurred through its reaction with starting bis(catechol)s **1**–**4** rather than through self-condensation.

Boronate ester assemblies **7**–**10** each display characteristically high extinction coefficients, and therefore UV/Vis and fluorescence spectra of dilute solutions (10^{-5} M in acetone) of each assembly could be obtained even though the same solutions had proven too dilute for the acquisition of well-resolved ^1H and ^{13}C NMR spectra: **7** (λ_{abs} = 328 nm, $\varepsilon = 2.1 \times 10^4$ $M^{-1}cm^{-1}$), **8** (λ_{abs} = 348 nm, $\varepsilon = 6.8 \times 10^4$ $M^{-1}cm^{-1}$), **9** (λ_{abs} = 327 nm, $\varepsilon = 3.5 \times 10^4$ $M^{-1}cm^{-1}$), and **10** (λ_{abs} = 348 nm, $\varepsilon = 4.3 \times 10^4$ $M^{-1}cm^{-1}$). All four assemblies showed significant fluorescence intensity, with **7** and **9** emitting in the violet region of the spectra (λ_{em} = 413 nm for both), and **8** and **10** emitting in the blue range at λ_{em} = 474 and 475 nm, respectively. The absorbance and fluorescence spectra of minimally soluble acetylene-linked assemblies (proposed structures **8** and **10**) are both red-shifted relative to biaryl assemblies **7** and **9** on account of the greater π-conjugation within their structures. Molecular modeling of the shape-persistent core of biaryl-linked boronate ester ovals **7** and **9** (see Figure S5 of the Supporting Information) predicts that the catechol and phenanthrene moieties twist ca 36.2° relative to each other. This biaryl twist causes the ovals to adopt a bowl-shaped conformation wherein the phenanthrene moieties of the assembly are tilted 144° with respect to the central plane of the assembly. All atoms within the shape-persistent core of the acetylene-linked assemblies, by contrast, are predicted to be coplanar.

Taken together the collective spectroscopic evidence is supportive of the formation of boronate ester ovals **7**–**10**. In particular, MALDI mass spectrometric analysis of assemblies **7** and **9** indicates that they are discrete boronate ester [2+2] assemblies. However both of these discrete boronate ester ovals are poorly soluble in common organic solvents. In the case of assemblies involving acetylene-linked bis(catechol)s **2** and **4**, neither hexyloxy nor DEG-CH_3 substituents are capable of providing sufficient solubility to balance the higher π-surface area of the polycyclic aromatic core of each assembly. The assemblies were found to be thermally robust as all four compounds display melting points above 200 °C.

Given the significant structural similarity between target boronate ester assemblies **7**–**10** and previously reported boronate ester rectangles (Scheme 1, c) it is both surprising and interesting to observe such a dramatic difference in the solubility of this new series of compounds relative to those previously studied. Within this series it appears that the increase in π-surface is the dominant influence limiting the solubility of proposed boronate ester assemblies **7**–**10**. Each of the target assemblies **7**–**10** possesses greater π-surface area at their core than the notably more soluble boronate ester rectangles. Only assemblies **7** and **9**, i.e. those with less overall π-surface area within a smaller shape-persistent core, could be definitively characterized by mass spectrometric analysis as being discrete boronate ester oval assemblies. The larger acetylene-linked assemblies (**8** and **10**) with greater π-surface area proved to be too insoluble for characterization by NMR or mass spectrometry. It is of interest to investigate whether functionalization of the phenanthrene moieties of biaryl- and acetylene-linked bis(catechol)s with larger solubilizing groups would be sufficient to overcome the observed insolubility imposed by their relatively large π-surface areas. Toward this aim, THB-substituted bis(catechol)s **5** and **6** (Figure 1) were synthesized and their assembly with **BDBA** was investigated.

Soluble Boronate Ester Assemblies

The synthetic route used to prepare phenanthrene bis(catechol)s **1**–**4** (Scheme 2, a) is easily adaptable to allow a variety of solubilizing groups to be incorporated at positions 9 and 10 of their phenanthrene moiety. In an attempt to prepare notably more soluble analogues of boronate ester assemblies **7**–**10**, 3,4,5-tris(hexyloxy) benzyl bromide **28**, a derivative of gallic acid (Scheme 2, b), was introduced. THB-functionalized bis(catechol)s **5** and **6** were synthesized upon reacting 3,6-dibromophenanthrene-9,10-diol (**15**) with benzyl bromide **28**.

Initial attempts to assemble THB-substituted boronate ester ovals **11** and **12** (Scheme 4, bottom) relied upon the same reaction conditions used to prepare assemblies of

BDBA with bis(catechol)s **1**–**4**, namely stirring an equimolar amount of **BDBA** and bis(catechol) derivative **5** or **6** at 50 °C in a 10:1 mixture of $CDCl_3$ and CD_3OD. ^1H NMR spectra recorded shortly after mixing (ca. 15 min) revealed significantly increased solubility of the species in solution. After 3 h of mixing the ^1H NMR spectrum remained highly complex and it was clear that multiple species, including a significant percentage of starting materials, were present in solution. It is a common characteristic of dynamic covalent self-assembly[1] that initial ^1H NMR spectra reveal multiple species as different oligomers and kinetic intermediates equilibrate toward a final, thermodynamically stable product. In the case of target boronate ester assemblies **11** and **12**, however, signals in each assemblies' ^1H NMR spectra did not sharpen as a function of time. These results were somewhat surprising given the overall structural similarities boronate ester ovals **11** and **12** share with assemblies **7** and **9**, which did collapse to give one predominant structure at equilibrium as indicated by ^1H NMR spectroscopy and MALDI mass spectrometry.

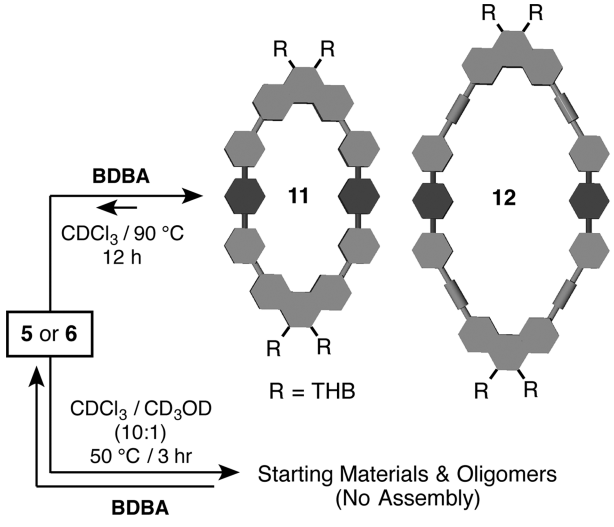

Scheme 4. Dynamic covalent assembly of THB-functionalized boronate ester ovals **11** and **12** from bis(catechol)s **5** and **6**, respectively, is achieved in $CDCl_3$. In a mixture of $CDCl_3/CD_3OD$ (10:1) gives only starting materials and oligomers.

The primary difference between assemblies **7** and **9** vs. **11** and **12** is the introduction of hexyloxy-substituted gallic acid derivatives. It was hypothesized that these larger solubilizing groups may have changed the solubility of bis(catechol) starting materials **5** and **6** so significantly that in a 10:1 mixture of $CDCl_3/CD_3OD$ the dynamic equilibrium is shifted toward starting materials and small oligomers bearing terminal –OH functionalities. To investigate this hypothesis further the self-assembly of boronate ester ovals **11** and **12** was attempted in pure $CDCl_3$. Returning to purely hydrophobic conditions and forgoing the catalytic methanol proved successful, and provided assemblies **11** and **12** in good yields (Scheme 4, top). The formation of boronate ester ovals **11** and **12** as dominant, though not necessarily exclusive, species in solution is supported by key shifts in their ^1H NMR spectra (Figure 3). Most notably, catechol –OH_α and –OH_β signals, which appear at δ = 6.1 and 5.8 ppm for bis(catechol) **6**, disappear upon assembly. The disappearance of catechol –OH signals is coincident with the emergence of singlet H_γ at δ = 7.96 ppm, which corresponds to the proton of **BDBA** in assembly **12**. Free **BDBA** and its corresponding anhydride are insoluble in chloroform, therefore appearance of an aromatic boronate ester signal around 7.96 ppm is strongly indicative of the assembly of **BDBA** with bis(catechol) **6**. Assembly is further supported by 0.6–0.3 ppm downfield shifts of aromatic catechol unit peaks. As can be seen in Figure 3 the ^1H NMR spectrum of assembly **12** is not cleanly resolved, showing evidence of baseline noise and the existence of trace signals not attributable to **12**. It is likely that minor quantities of alternative assemblies are present at equilibrium, as is often the case in dynamic combinatorial libraries. The intensity of signals corresponding to **12**, however, suggests that it is the dominant species at equilibrium. Analogous changes were observed for the formation of boronate ester oval assembly **11** (see Figure S1 of the Supporting Information).

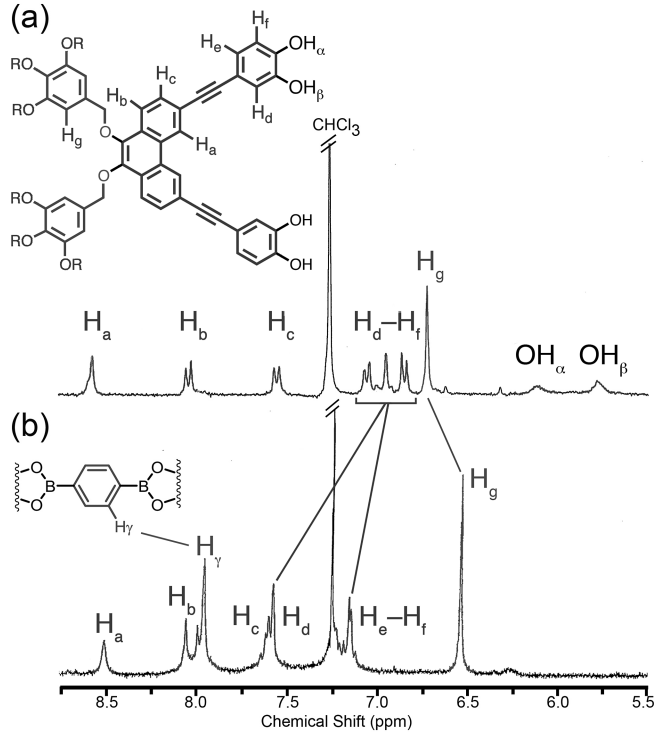

Figure 3. Partial ^1H NMR spectra ($CDCl_3$, 400 MHz, 298 K) of THB-functionalized bis(catechol) **6** (a) and boronate ester assembly **12** (b) indicating shifts of diagnostic proton signals observed upon self-assembly.

The sensitivity of boronate ester ovals **11** and **12** to protic solvents was further investigated by adding increasing equivalents of CD_3OD to a $CDCl_3$ solution of each assembly. The resulting ^1H NMR spectra became disordered upon the addition of 10 equiv. of CD_3OD, and continued to increase in disorder until the dynamically equilibrating species had fully reverted to starting materials by 50 equiv. of CD_3OD (see Figure S2 of the Supporting Information). For comparison, initial attempts to self-assemble boronate

ester ovals **11** and **12** in a mixture of 10:1 $CDCl_3/CD_3OD$ corresponded to approximately 1000 equiv. of CD_3OD, far exceeding the 50 equiv. found sufficient to favor disassembly. This observation is in direct contrast to sparingly soluble boronate ester assemblies **7** and **9**, which showed no indication of product formation in pure $CDCl_3$ and prolonged stability in 10% CD_3OD. For additional comparison, the closely related boronate ester rectangle assemblies (Scheme 1, c) could only be reverted to starting materials by refluxing in a mixture of 1:1 D_2O/CD_3OD.[29] These observations provided additional evidence that the 3,4,5-tris-(hexyloxy)benzyl substituents of bis(catechol) derivatives **5** and **6** both increase the solubility of boronate ester assemblies **11** and **12** while also decreasing their stability in the presence of protic solvents.

Further support for the formation of boronate ester ovals was obtained by IR spectroscopy. Strong intensity bands were observed at 1225, 1063, 638 cm^{-1} (oval **11**) and at 1222, 1050, and 659 cm^{-1} (oval **12**). These three IR bands are characteristic[32] of boronate esters and correspond to symmetric C–O stretching, B–O stretching, and out-of-plane displacement of boron and oxygen atoms within the boronate ester C_2O_2B ring. These IR results are consistent with the observed results for minimally soluble ovals **7**–**10**. The UV/Vis and fluorescence spectra (10^{-5} M in $CHCl_3$) were also found to be comparable with the results obtained for assemblies **7**–**10**, with high extinction coefficients for assemblies **11** (332 nm, $\varepsilon = 4.2 \times 10^4$ $M^{-1}cm^{-1}$) and **12** (λ_{abs} = 353 nm, $\varepsilon = 3.7 \times 10^4$ $M^{-1}cm^{-1}$), and emission in the blue region of the visible spectrum (**11**, λ_{em} = 394 nm and **12**, λ_{em} = 409 nm).

As discussed previously, ^{1}H NMR and IR spectroscopy alone cannot rule out the formation of highly symmetric boronate ester oligomers as opposed to discrete assemblies. Mass spectrometry was attempted to quantitatively establish the molecularity of proposed boronate ester ovals **11** and **12**. Unfortunately, despite considerable effort, mass spectral analysis of both assemblies by MALDI and electrospray ionization, both considered generally "soft" ionization techniques, revealed only starting materials and fragments. In general, all investigations of proposed assemblies **11** and **12** have shown that they are significantly more labile than related boronate ester assemblies **7**–**10** and previously studied boronate ester rectangles. Differential scanning calorimetry (DSC) and melting point analyses of all six boronate ester assemblies also indicate that THB-substituted assemblies **11** and **12** are less thermally stable than hexyloxy and DEG-CH_3 functionalized assemblies **7**–**10**. DSC traces of **11** revealed sudden decomposition, without a coherent melt, at 195 °C. Similarly, assembly **12** was observed to decompose at 185 °C. By comparison, the less soluble assemblies **7**–**10** were each stable well above 200 °C. It is believed that the general lability of highly functionalized assemblies **11** and **12** is the primary factor underlying in the difficulty of obtaining mass spectra of the discrete assemblies. It is of course possible that the proposed boronate ester assemblies **11** and **12** are not in fact discrete and are instead mixtures of various oligomers. Such oligomers would have near identical IR spectra as boronate ester ovals **11** and **12**. However, it is believed that the proposed discrete assemblies **11** and **12** are the principle, thermodynamic species in solution given that initially complex mixtures of dynamically equilibrating species collapse to form a dominant, well-defined final structure observed by ^{1}H NMR spectroscopy.

Model of Boronate Ester Assembly Formation

Analysis of THB-functionalized boronate ester assemblies **11** and **12** indicates that sufficiently large solubilizing groups are able to overcome the general insolubility observed for assemblies **7**–**10**. Within this series of compounds, however, increased solubility comes at the cost of increased lability in the presence of protic solvents. Collectively, the results presented herein help build a better understanding the varying roles solubility, functionality, and reaction conditions can play in the self-assembly, isolation, and characterization of shape-persistent boronate ester assemblies. Shown in Figure 4 is a model that summarizes these roles within the context of the current research.

In Figure 4 different pathways potentially leading to the formation of discrete, shape-persistent boronate ester assemblies are indicated by different equilibrium arrows: dashed arrows represent unproductive pathways while solid arrows indicate pathways that may lead to assembly formation. Furthermore, bold arrows indicate precipitation, which removes species from dynamic covalent libraries (DCLs) and can contribute to driving equilibria in a given direction. As can be seen in the Figure different reaction conditions allow entrance into the dynamically equilibrating libraries of species depending on the functionality of bis(catechol) SBUs. Less soluble hexyloxy and DEG-CH_3-substituted species **1**–**4** are prevented from entering into a DCL when mixed with **BDBA** in pure chloroform, even at elevated temperatures. The addition of 10% CD_3OD, however, provides the sufficient solubility. In the case of THB-substituted bis(catechol)s **5** and **6**, however, the presence of CD_3OD shifts the equilibrium too far toward starting materials thus preventing productive dynamic covalent exchange. In the absence of CD_3OD, the thermodynamics (and therefore equilibrium) shift back toward the assembly of **5** and **6** with **BDBA**.

Finding productive pathways out of a dynamically converting mixture of intermediates is of equal importance to successful assembly formation. When and how readily a given assembly is removed from of a DCL, potentially driven by precipitation or aggregation, is especially important. Precipitation rates and pathways influence crystal growth and quality, the ability to form co-assemblies and co-crystals, and underlie the (unproductive) precipitation of undesired kinetic intermediates. Assemblies involving acetylene-linked bis(catechol)s **2** and **4**, for example, are so poorly soluble that they readily precipitate out of solution. It is believed that a primary driving force for precipitation is the formation of closed, discrete macrocycles that (i) lack

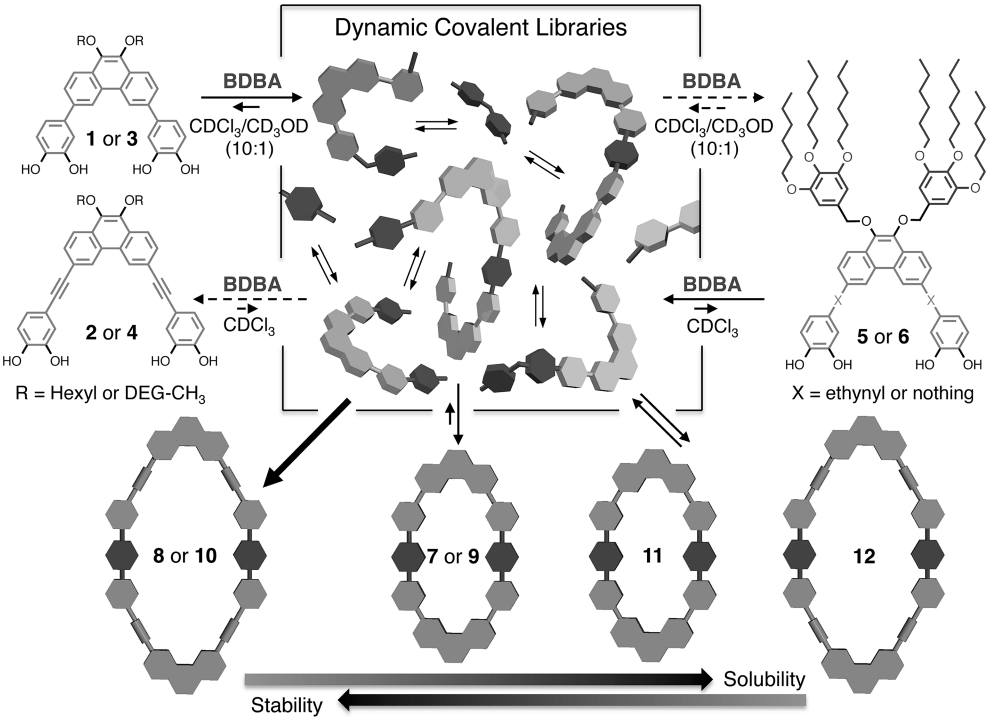

Figure 4. Generalized model of the varying pathways that favour the dynamic assembly of boronate ester assemblies and how differences in SBU structure and reaction conditions influence self-assembly.

any hydroxy functionalities and (ii) are able to interact and aggregate[33] through aromatic stacking interactions. The planar, acetylene-conjugated assemblies formed from **2** and **4** are therefore observed to be the least soluble of the series investigated. Assemblies formed between biaryl bis(catechol)s **1** and **3** with **BDBA** display a more productive balance wherein their low solubility aids in pulling discrete species out of solution while biaryl twisting disrupts intramolecular π-stacking and aggregation. The resulting assemblies **7** and **9** are therefore stable enough to withstand hydrolysis (equilibrium favoring products) yet still soluble enough to characterize.

The greatly increased solubility of THB-substituted bis(catechol)s **5** and **6**, however, renders their resulting assemblies with **BDBA** highly labile to disassembly in protic solvents. The equilibrium between dynamically interconverting species and discrete assemblies **11** and **12** is tenuous and readily favors starting materials and small oligomers in the presence of trace water or methanol. It is therefore observed that significantly increasing solubility, while helpful in providing pathways into DCLs, can actually limit the ability to form and characterize discrete boronate ester assemblies. Such highly soluble and readily labile assemblies are less likely to drive dynamically converting equilibria toward a desired product by precipitation or aggregation processes. This subtle balance between the solubility and stability of discrete assemblies directly influences some of their most valuable attributes, namely their ability to form stable, higher-order aggregates in solution, on surfaces, and within materials applications. While Figure 4 is drawn specifically in relation to results gathered in the current study it is likely that similar models can be applied to other discrete covalent organic polygons and, potentially, the synthesis and isolation of covalent organic frameworks.

Conclusions

The results presented herein suggest that the balance between SBU solubility, assembly formation, and assembly stability can be highly sensitive. This research builds upon recent related work where seemingly subtle differences in functionality can dramatically influence the success or failure of obtaining discrete, shape-persistent boronate ester (or boroxine anhydride) assemblies. In order to fully develop the chemistry and applications of discrete boronate ester assemblies it is necessary to obtain a better understanding of the many factors that determine (i) whether discrete assemblies will form, (ii) to what extent such assemblies will form, and (iii) under what conditions such assemblies will remain stable. Understanding the roles that functionality, solubility, and stability play in the assembly of discrete boronate ester COPs can be expected to also contribute to the optimization of reaction conditions used to synthesize related COFs. Without a thorough understanding of the experimental and structural influences that underlie the assembly of discrete boronate ester polygons/polyhedra, and infinite boronate ester COFs, it can be expected that the discovery of new frameworks and the optimization of their synthesis will largely be an effort of trial and error. The results presented herein hope to chart some small, yet important, steps toward a better understanding

of boronate ester self-assembly with the ultimate goal of more judicious, de novo design and synthesis of new shape-persistent boronate ester framework assemblies, both discrete and infinite.

Experimental Section

General: Chemicals were obtained from commercial sources and used as purchased. Reagent-grade solvents were used as obtained from commercial sources. Anhydrous solvents were dried using an Innovative Technologies SPS-400-5 solvent purification system. ^{1}H and ^{13}C NMR spectra were recorded with a Varian Mercury (300 MHz and 75 MHz, respectively) spectrometer using residual solvent as the internal standard. All chemical shifts are quoted using the δ scale and all coupling constants are expressed in Hertz [Hz]. Infrared spectroscopic analysis was performed on a Perkin–Elmer Spectrum BX FT-IR system. UV/Vis spectroscopy was recorded on a Varian Cary 100 Bio UV/Vis spectrophotometer. Differential scanning calorimetry (DSC) was performed on a TA Instruments DSC Q20 equipped with an RCS90 cooling system and were acquired at rates of 10 °C min^{-1} (heating) and 5 °C min^{-1} (cooling). ESI/APCI-MS and MALDI-MS analyses were carried out at the University of California, Riverside, Mass Spectrometry Facility.

Compound 28: To a solution of triphenylphosphine (6.3 g, 24.10 mmol) in dichloromethane (80 mL) was added carbon tetrabromide (4.0 g, 12.05 mmol). A solution was prepared of **27**[34] (4.9 g, 12.05 mmol) in dichloromethane (24 mL), which was added to the stirring triphenylenephosphine and carbon tetrabromide solution at 0 °C. The reaction was stirred at 0 °C for 1.5 h, at which point water was added (150 mL), and the crude product extracted with chloroform (3 × 100 mL). The combined organic layers were washed with brine (150 mL), dried with $MgSO_4$, and concentrated under reduced pressure. The crude residue was purified using a pad of silica, eluting with 1:1 hexanes/dichloromethane, affording pure **28** as a colourless oil (4.7 g, 83%). ESI/APCI (*m*/*z*) $[MH]^+$ calculated for $C_{25}H_{44}O_3Br$, 471.2468, found 471.2464. ^{1}H NMR ($CDCl_3$, 300 MHz): δ = 6.58 (s, 2 H), 4.45 (s, 2 H), 4.00–3.92 (m, 6 H), 1.85–1.74 (m, 6 H), 1.50–1.46 (m, 6 H), 1.35–1.33 (m, 12 H), 0.96–0.89 (m, 9 H) ppm. ^{13}C NMR ($CDCl_3$, 75 MHz): δ = 153.2, 132.3, 107.0, 73.4, 69.1, 47.0, 31.7, 31.5, 30.2, 29.3, 25.7, 22.6, 14.0 ppm.

General Method for the Preparation of Dibromophenanthrene Derivatives 16–18: To a mixture of **15**,[35] the appropriate alkyl halide or tosylate (3 equiv.), potassium carbonate (4–6 equiv.), 18-crown-6 (catalytic), and lithium bromide (catalytic) were added under an inert atmosphere in a minimum amount of dry dimethylformamide. The reaction solution was stirred at 80 °C overnight, cooled, and poured over water. The organic material was extracted (3 ×) with an organic solvent, and the combined organic layers washed twice with water, dried with $MgSO_4$, and concentrated under reduced pressure. The crude product was purified by flash chromatography.

Compound 16: The crude product was extracted with hexanes and eluted from the column with 10% dichloromethane in hexanes. Reaction scale: **15** (0.8 g, 2.17 mmol), yield (0.9 g, 82%). Spectroscopic characterization matched that reported in the literature.[35]

Compound 17: The crude compound was extracted with ethyl acetate and eluted from the column with 3:1 hexanes/ethyl acetate, affording a pale yellow oil that gradually solidified. Reaction scale: **15** (313 mg, 0.85 mmol), yield (410 mg, 88% yield), m.p. 55.7–56.6 °C. APCI-MS (*m*/*z*) $[M + H]^+$ calculated for $C_{24}H_{29}O_6Br_2$, 571.0325, found 571.0334. ^{1}H NMR ($CDCl_3$, 300 MHz): δ = 8.65 (s, 2 H), 8.26 (d, *J* = 9.4 Hz, 2 H), 7.71 (d, *J* = 11.4 Hz, 2 H), 4.43–4.39 (m, 4 H), 3.88–3.84 (m, 4 H), 3.72–3.69 (m, 4 H), 3.61–3.58 (m, 4 H), 3.42 (s, 6 H) ppm. ^{13}C NMR ($CDCl_3$, 75 MHz): δ = 142.9, 130.5, 128.9, 128.5, 125.2, 124.7, 120.5, 72.4, 72.0, 70.5, 70.4, 59.1 ppm.

Compound 18: The crude product was extracted with hexanes, and eluted from the column with 1:1 dichloromethane/hexanes, affording the pure product as yellow solid. Reaction scale: **15** (135 mg, 0.368 mmol), (261 mg, 62%), m.p. 73–75 °C. ESI/APCI (*m*/*z*) $[MNH_4]^+$ calculated for $C_{64}H_{96}NO_8Br_2$, 1164.5497, found 1164.5459. ^{1}H NMR ($CDCl_3$, 300 MHz): δ = 8.65 (s, 2 H), 8.06 (d, *J* = 8.8 Hz, 2 H), 7.66 (d, *J* = 9.7 Hz, 2 H), 6.6.4 (s, 4 H), 5.20 (s, 4 H), 3.94 (t, *J* = 6.0 Hz, 4 H), 3.88 (t, *J* = 6.7 Hz, 8 H), 1.79–1.70 (m, 12 H), 1.51–1.40 (m, 12 H), 1.38–1.29 (m, 24 H), 0.92 (t, *J* = 6.3 Hz, 18 H) ppm. ^{13}C NMR ($CDCl_3$, 75 MHz): δ = 153.2, 143.1, 138.2, 131.9, 130.4, 128.8, 128.5, 125.3, 120.6, 106.8, 75.8, 73.4, 69.1, 31.7, 31.5, 30.2, 25.7, 22.6, 14.0 ppm.

General Procedure for Preparing Diaryl-Substituted Phenanthrenes 21–23: To a heavy walled glass vessel was added phenanthrene dihalide, **14** (2.5 equiv.), and potassium phosphate (4 equiv.). The flask was flushed with nitrogen, and palladium(II) acetate (2 mol-%) and SPhos ligand (4 mol-%) were added. The flask was purged and backfilled with nitrogen (3 ×), and degassed toluene and water (10:1, 0.5 M with respect to phenanthrene) were added. The flask was sealed with a Teflon® screw-cap and stirred at 100 °C overnight. The reaction suspension was cooled and filtered through Celite, eluting with dichloromethane. The filtrate was concentrated under reduced pressure and purified via column chromatography.

Compound 21: Note: for this compound, Sphos Palladacycle (4 mol-%) was used in place of palladium(II) acetate and Sphos ligand. Similarly, potassium carbonate (4 equiv.) was used in place of potassium phosphate. The product eluted with 10:1 hexanes/dichloromethane, and the pure product isolated as an white solid. Reaction scale: **16** (404 mg, 0.712 mmol), yield (753 mg, 99% yield). (Note: **21** has also been isolated using the same reaction conditions as **22**, with a lower yield of 50%) M.p. 104.9–105.7 °C. APCI-MS (*m*/*z*) $[M + H]^+$ calculated for $C_{62}H_{99}O_6Si_4$, 1051.6513, found 1051.6511. ^{1}H NMR ($CDCl_3$, 300 MHz): δ = 8.81 (s, 2 H), 8.27 (d, *J* = 8.5 Hz, 2 H), 7.79 (d, *J* = 8.5 Hz, 2 H), 7.31–7.23 (m, 4 H), 6.97 (d, *J* = 7.6 Hz, 2 H), 4.24 (t, *J* = 12 Hz, 4 H), 1.99–1.89 (m, 4 H), 1.64–1.57 (m, 4 H), 1.44–1.39 (8 H), 1.05 (s, 18 H), 1.04 (s, 18 H), 0.95 (t, *J* = 6.0 Hz, 6 H), 0.29 (s, 12 H), 0.27 (s, 12 H) ppm. ^{13}C NMR ($CDCl_3$, 75 MHz): δ = 147.1, 146.6, 143.1, 138.1, 134.8, 128.8, 128.6, 125.8, 122.8, 121.4, 120.4, 120.3, 73.7, 31.7, 30.5, 25.9, 22.7, 18.6, 14.1, –4.0 ppm.

Compound 22: The product eluted with 12:1 dichloromethane/ethyl acetate, affording **22** as a pale yellow solid Reaction scale: **17** (365 mg, 0.638 mmol), yield (623 mg, 90% yield), m.p. 89.4–92.3 °C. APCI-MS (*m*/*z*) $[M + Na]^+$ calculated for $C_{60}H_{94}O_{10}NaSi_4$, 1109.5816, found 1109.5851. ^{1}H NMR ($CDCl_3$, 300 MHz): δ = 8.80 (s, 2 H), 8.32 (d, *J* = 8.5 Hz, 2 H), 7.73 (dd, *J* = 8.5, 1.5 Hz, 2 H), 7.43–7.09 (m, 8 H), 6.83 (d, *J* = 8.2 Hz, 2 H), 4.46–4.43 (m, 4 H), 3.90–3.87 (m, 4 H), 3.74–3.71 (m, 4 H), 3.63–3.60 (m, 4 H), 3.43 (s, 6 H), 1.03 (s, 18 H), 1.01 (s, 18 H), 0.27 (s, 12 H), 0.24 (s, 12 H) ppm. ^{13}C NMR ($CDCl_3$, 75 MHz): δ = 147.1, 146.7, 142.8, 138.3, 134.8, 132.1, 129.5, 128.9, 128.4, 125.8, 123.5, 123.2, 121.4, 120.4, 120.3, 72.4, 72.1, 70.6, 59.1, 26.1, 18.6, –4.0 ppm.

Compound 23: The pure product eluted from the column in pure dichloromethane. Reaction Scale: **18** (230 mg, 0.200 mmol), yield (157 mg, 47%), yellow solid, m.p. 55–57 °C. ESI/APCI (*m*/*z*) [MNa] + calculated for $C_{100}H_{158}O_{12}NaSi_4$, 1686.0723, found 1686.0682. ^{1}H NMR ($CDCl_3$, 300 MHz): δ = 8.83 (s, 2 H), 8.28 (d, *J* = 8.5 Hz,

2 H), 7.77 (d, J = 8.5 Hz, 2 H), 7.27–7.22 (m, 4 H), 6.97 (d, J = 7.9 Hz, 2 H), 7.75 (s, 4 H), 5.5 (s, 4 H), 3.99–3.91 (m, 12 H), 1.82–1.71 (m, 12), 1.54–1.41 (m, 12 H), 1.39–1.27 (m, 24 H), 1.06 (s, 18 H), 1.05 (s, 18 H), 0.95–0.86 (m, 18 H), 0.29 (s, 12 H), 0.28 (s, 12 H) ppm. ^{13}C NMR ($CDCl_3$, 75 MHz): δ = 153.2, 147.2, 146.7, 143.1, 138.4, 138.0, 134.7, 132.5, 129.0, 128.3, 125.8, 123.0, 121.4, 120.4, 120.3, 106.6, 75.8, 73.4, 69.1, 31.8, 31.6, 30.3, 29.4, 26.0, 25.8, 22.6, 18.5, 14.0, –4.0 ppm.

General Procedure for Preparing Ethynyl-Spaced Phenanthrenes 24–26: To a nitrogen-charged Schlenk flask was added 9,10-disubstituted 3,6-dibromophenanthrene (1 equiv.), **20** (3 equiv.), and triphenylphosphine (0.2 equiv.). To the mixture was added *trans*-dichlorobis(triphenylphosphine)palladium (0.1 equiv.), and copper iodide (0.2 equiv.) in that order. The flask was evacuated, purged with nitrogen, and wrapped in foil. To the reaction flask was added dry, degassed piperidine and tetrahydrofuran (0.27 M and 0.125*M* with respect to phenanthrene), and the reaction stirred for ca. 65 h, at which point water was added, and the product extracted with an organic solvent. The combined organic layers were washed with brine, dried with $MgSO_4$, and concentrated under reduced pressure. The crude product was purified by column chromatography.

Compound 24: The crude product was extracted with dichloromethane, and eluted from the column in 10% dichloromethane in hexanes. Reaction scale: **16** (177 mg, 0.331 mmol), yield 160 mg (0.145 mmol, 44%). The product was isolated as a yellow oil. APCI-MS (m/z) $[M]^+$ calculated for $C_{66}H_{98}O_6Si_4$, 1096.6435, found 1098.6437. ^{1}H NMR ($CDCl_3$, 300 MHz): δ = 8.80 (s, 2 H), 8.19 (d, J = 8.2 Hz, 2 H), 7.73 (d, J = 8.2 Hz, 2 H), 7.13–7.08 (m, 4 H), 6.83 (d, J = 8.2 Hz, 2 H), 4.22 (t, J = 7.3 Hz, 4 H), 1.96–1.87 (m, 4 H), 1.63–1.58 (m, 4 H), 1.43–1.36 (m, 8 H), 1.03 (s, 18 H), 1.01 (s, 18 H), 0.94 (t, J = 7.3 Hz, 6 H), 0.27 (s, 12 H), 0.24 (s, 12 H) ppm. ^{13}C NMR ($CDCl_3$, 75 MHz): δ = 148.0, 146.8, 143.7, 129.8, 129.2, 127.9, 126.0, 125.6, 124.2, 122.4, 121.1, 120.9, 116.1, 90.2, 88.4, 73.8, 31.7, 30.4, 25.9, 22.7, 18.5, 14.1, –4.0 ppm.

Compound 25: The crude product was extracted with ethyl acetate, and eluted from the column in 5% ethyl acetate in dichloromethane. Reaction Scale: **17** (1.4 g, 2.45 mmol), yield 695 mg (0.612 mmol, 25%). The product was isolated as a dark oil. APCI-MS (m/z) $[M + Na]^+$ calculated for $C_{64}H_{94}O_{10}NaSi_4$, 1157.5816, found 1157.5848. ^{1}H NMR ($CDCl_3$, 300 MHz): δ = 8.80 (s, 2 H), 8.82 (d, J = 8.5 Hz, 2 H), 7.73 (d, J = 8.5 Hz, 2 H), 7.13–7.08 (m, 4 H), 6.84 (d, J = 8.2 Hz, 2 H), 4.46–4.43 (m, 4 H), 3.90–3.86 (m, 4 H), 3.74–3.71 (m, 4 H), 3.63–3.60 (m, 4 H), 3.43 (s, 6 H), 1.03 (s, 18 H), 1.01 (s, 18 H), 0.27 (s, 12 H), 0.24 (s, 12 H) ppm. Low solubility precluded the collection of a well-resolved ^{13}C NMR spectrum.

Compound 26: The reaction was not extracted, but instead was filtered through Celite, eluting with dichloromethane. The filtrate was concentrated under reduced pressure, and the crude material purified by column chromatography, eluting with 1:1 hexanes/dichloromethane, affording pure **26** as a yellow semisolid. Reaction scale: **18** (120 mg, 0.104 mmol), yield (93 mg, 52%). ESI/APCI (m/z) $[M + Na]^+$ calculated for $C_{104}H_{158}O_{12}NaSi_4$, 1734.0723, found 1734.0746. ^{1}H NMR ($CDCl_3$, 300 MHz): δ = 8.81 (s, 2 H), 8.17 (d, J = 8.6 Hz, 2 H), 7.70 (d, J = 8.6 Hz, 2 H), 7.16–7.08 (m, 4 H), 6.84 (d, J = 8.2 Hz, 2 H), 6.69 (s, 4 H), 5.23 (s, 4 H), 3.99–3.87 (m, 12 H), 1.80–1.74 (m, 12 H), 1.54–1.42 (m, 12 H), 1.36–1.30 (m, 24 H), 1.04 (s, 18 H), 1.01 (s, 18 H), 0.93–0.89 (m, 18 H), 0.27 (s, 12 H), 0.25 (s, 12 H) ppm. ^{13}C NMR ($CDCl_3$, 75 MHz): δ = 153.2, 148.0, 146.8, 138.2, 132.2, 129.8, 129.0, 128.1, 126.0, 125.6, 124.2, 122.6, 121.3, 121.1, 116.0, 106.9, 90.4, 88.3, 75.8, 73.4, 69.1, 31.8, 31.6, 30.3, 29.3, 26.0, 25.8, 22.6, 14.0, –4.1 ppm.

General Procedures for the Deprotection of TBDMS Groups to Afford Phenanthrene-Bis(catechol)s 1–6. Method I: To a solution of TBDMS-protected phenanthrene monomer dissolved in dry dimethylformamide (0.1 M with respect to phenanthrene) was added potassium fluoride (8 equiv.), followed by concentrated hydrobromic acid (0.6 equiv.). The reaction was monitored by TLC and stirred overnight, at which point 2 M HCl was added (excess), and the product extracted with an organic solvent. The combined organic layers were washed with brine, dried with $MgSO_4$, and concentrated under reduced pressure. The crude product was purified by column chromatography. Note: yields were not optimized for phenanthrene deprotections.

Method II: To a given TBDMS-protected phenanthrene derivative was added an excess of tetraethylene-glycol (80 equiv.). Tetrahydrofuran was slowly added, with stirring, until reaction became homogeneous. Potassium fluoride (8 equiv.) was added, provoking an immediate color change. The reaction was monitored by thin layer chromatography, and was complete within 30 min. Water was added, and the product extracted with diethyl ether. The combined organic layers were washed with water and brine. The combined aqueous layers were back extracted with diethyl ether, and the combined organic layers dried with $MgSO_4$ and concentrated under reduced pressure. The residue was purified by column chromatography. The low solubility of compounds **2**, **3**, **4**, and **6** made chromatographic purification nontrivial, significantly impacting product yields. For bis(catechol)s **1**–**6** carbon spectra were omitted due to very low solubility resulting in little to no discernible signal above baseline noise.

Compound 1 (isolated using Method I): To quench the reaction, 20 mL 2 M HCl was added, and the crude product was extracted with diethyl ether. The pure product eluted from the column with 100% ethyl acetate. Reaction Scale: **21** (570 mg, 0.542 mmol), yield 274 mg (0.461 mmol, 85%). The product was isolated as a lavender solid, m.p. 148–154 °C. APCI-MS (m/z) $[M]^+$ calculated for $C_{38}H_{42}O_6$, 594.2976, found 594.2995 (ppm error = 3.2). ^{1}H NMR ($CO(CD_3)_2$, 300 MHz): δ = 9.01 (s, 2 H), 8.28 (d, J = 8.8 Hz, 2 H), 8.08 (s, 2 H), 8.04 (s, 2 H), 7.88 (dd, J = 8.8, 1.8 Hz, 2 H), 7.40 (d, J = 2.4 Hz, 2 H), 7.27 (dd, J = 8.2, 2.4 Hz, 2 H), 6.99 (d, J = 8.2 Hz, 2 H), 4.26 (t, J = 6.4 Hz, 4 H), 2.00–1.91 (m, 4 H), 1.69–1.59 (m, 4 H), 1.47–1.36 (m, 8 H), 0.94 (t, J = 7.3 Hz, 6 H) ppm.

Compound 2 (isolated using Method I): Instead of dimethylformamide, the solvent used for this reaction was a 2:1 solution of tetrahydrofuran:dimethylformamide. To quench the reaction, 10 mL of 2*M* HCl was added, and the crude product was extracted with diethyl ether. The pure product eluted from the column with 1:1 hexanes/ethyl acetate. Reaction Scale: **24** (158 mg, 0.144 mmol), yield 50 mg (0.078 mmol, 54%). The product was isolated as a purple solid, m.p. 131–133 °C (note, the dark, oily nature of this material makes observing the melting point difficult). APCI-MS (m/z) $[M + H]^+$ calculated for $C_{42}H_{43}O_6$, 643.3054, found 643.3063. ^{1}H NMR ($CO(CD_3)_2$, 300 MHz): δ = 8.94 (s, 2 H), 8.31 (s, 4 H), 8.24 (d, J = 8.5 Hz, 2 H), 7.74 (d, J = 8.5 Hz, 2 H), 7.12 (d, J = 1.8 Hz, 2 H), 7.04 (dd, J = 8.2, 1.8 Hz, 2 H), 6.88 (d, J = 7.9 Hz, 2 H), 4.23 (t, J = 6.6 Hz, 4 H), 1.97–1.88 (m, 4 H), 1.65–1.55 (m, 4 H), 1.43–1.38 (m, 8 H), 0.92 (t, J = 6.9 Hz, 6 H) ppm.

Compound 3 (isolated using Method I): To quench the reaction, 20 mL of 2*M* HCl was added, and the crude product was extracted with ethyl acetate. The pure product eluted from the column with 100% ethyl acetate. Reaction Scale: **22** (620 mg, 0.570 mmol), yield (161 mg, 45%). Product was isolated as dark red oil. APCI-MS (m/z) $[M + Na]^+$ calculated for $C_{36}H_{38}O_{10}Na$, 653.2357, found 653.2346 (ppm error = –1.7). ^{1}H NMR ($CO(CD_3)_2$, 300 MHz): δ

= 9.01 (s, 2 H), 8.45 (d, J = 8.8 Hz, 2 H), 8.10 (s, 2 H), 8.05 (s, 2 H), 7.88 (dd, J = 8.5, 1.5 Hz, 2 H), 7.40 (d, J = 2.1 Hz, 2 H), 7.29 (dd, J = 8.2, 2.1 Hz, 2 H), 6.99 (d, J = 8.2 Hz, 2 H), 4.46–4.43 (m, 4 H), 3.92–3.89 (m, 4 H), 3.72–3.69 (m, 4 H), 3.59–3.56 (m, 4 H), 3.35 (s, 6 H) ppm.

Compound 4 (isolated using Method I): To quench the reaction, 30 mL of 2 M HCl was added, and the crude product was extracted with dichloromethane. The pure product eluted from the column with 1:1 acetone/hexanes. Reaction Scale: **25** (690 mg, 0.608 mmol), isolated yield (33 mg, 12%). The product was isolated as a dark solid, m.p. 93–94 °C (note, the dark, oily nature of this material makes observing the melting point difficult). APCI-MS (m/z) [M + H]$^+$ calculated for $C_{42}H_{37}O_{10}$, 701.2381, found 701.2370. ^{1}H NMR ($CO(CD_3)_2$, 300 MHz): δ = 8.92 (s, 2 H), 8.40 (d, J = 8.5 Hz, 2 H), 8.31 (s, 4 H), 7.72 (d, J = 8.5 Hz, 2 H), 7.10 (d, J = 1.8 Hz, 2 H), 7.02 (dd, J = 8.2, 1.9 Hz, 2 H), 6.86 (d, J = 7.9 Hz, 2 H), 4.43–4.40 (m, 4 H), 3.86–3.84 (m, 4 H), 3.67–3.64 (m, 4 H), 3.54–3.51 (m, 4 H), 3.31 (s, 6 H) ppm.

Compound 5 (isolated using Method II): The pure product eluted with 25% diethyl ether in dichloromethane as a dark yellow solid. Reaction scale: **23** (153 mg, 0.092 mmol), yield (89 mg, 80%). Decomposition: 125–135 °C. ESI/APCI (m/z) [M + Na]$^+$ calculated for $C_{78}H_{102}O_{12}Na$, 1229.7264, found 1229.7233. ^{1}H NMR ($CDCl_3$, 300 MHz, 0.05 M, chemical shifts of several aromatic signals were found to vary with concentration): δ = 8.40 (s, 2 H), 8.20 (d, J = 8.5 Hz, 2 H), 7.60 (d, J = 8.1 Hz, 2 H), 7.12–6.86 (m, 6 H), 6.71 (2 H), 6.51 (s, 4 H), 5.50 (2 H), 4.47 (s, 4 H), 4.04 (t, J = 6.6 Hz, 4 H), 3.79 (t, J = 6.4 Hz, 8 H), 1.86–1.78 (m, 12 H), 1.74–1.66 (m, 12 H), 1.41–1.26 (m, 24 H), 0.91 (t, J = 6.7 Hz, 18 H) ppm. ($CO(CD_3)_2$, 300 MHz): δ = 9.01 (s, 2 H), 8.29 (d, J = 8.5 Hz, 2 H), 8.06 (s, 4 H), 7.85 (d, J = 8.5 Hz, 2 H), 7.39 (s, 2 H), 7.26 (dd, J = 7.9, 2.2 Hz, 2 H), 7.0 (d, J = 7.9 Hz, 2 H), 6.83 (s, 4 H), 5.27 (s, 4 H), 3.94–3.88 (m, 12 H), 1.77–1.66 (m, 12 H), 1.56–1.40 (m, 12 H), 1.39–1.27 (m, 24 H), 0.89 (t, J = 6.5 Hz, 18 H) ppm.

Compound 6 (isolated using Method II): The product was extracted with ethyl acetate, and eluted from the column with 10% diethyl ether in dichloromethane, affording 6 as a dark yellow solid Reaction Scale: **26** (130 mg, 0.076 mmol), yield (41 mg, 43%). Decomposes at 199 °C. ESI/APCI (m/z) [M + Na]$^+$ calculated for $C_{78}H_{102}O_{12}Na$, 1229.7264, found 1229.7233. ^{1}H NMR ($CDCl_3$, 300 MHz, 0.05 M): δ = 8.59 (s, 2 H), 8.05 (d, J = 8.5 Hz, 2 H), 7.56 (d, J = 7.9 Hz, 2 H), 7.08–6.84 (m, 6 H), 6.73 (s, 4 H), 6.11 (s, 2 H), 5.78 (s, 2 H), 5.15 (s, 4 H), 3.99 (t, J = 5.6 Hz, 4 H), 3.90 (t, J = 6.4 Hz, 8 H), 1.80–1.70 (m, 12 H), 1.53–1.49 (m, 12 H), 1.37–1.26 (m, 24 H), 0.90 (t, J = 5.9 Hz, 18 H) ppm.

Conditions to Afford Phenanthrene Assemblies 7–12. Method I: To a mixture of organic tetra-ol (1 equiv.) and 1,4-benzenediboronic acid (1 equiv.) was added 10:1 chloroform/methanol (chloroform 0.01 M with respect to reagents). The reaction solution was stirred at 50 °C for 3 h at which point 4 Å molecular sieves were added, and the reaction stirred overnight at room temperature. The reaction mixture was dried with $MgSO_4$, filtered (rinsing with acetone), and the solvents removed via rotary evaporation. The solid residue was subjected to high vacuum at 90 °C for 1 h to afford solvent free assemblies.

Method II: A suspension was prepared of organic tetra-ol (1 equiv.) and 1,4-benzenediboronic acid (1 equiv.) in $CDCl_3$ (0.002 M) and refluxed at 90 °C overnight. The resulting solution was cooled, passed through a Teflon® syringe filter, and concentrated under reduced pressure to afford the desired assembly. For assemblies **7**–**12** carbon spectra could not be obtained because of their insolubility.

Assembly 7 (isolated using Method I): Reaction Scale: 1 (17.0 mg, 0.029 mmol), yield 18.8 mg (95%). The product was isolated as a grey solid that was sparingly soluble in acetone, m.p. > 200 °C. IR (powder, ATR): $\tilde{\nu}$ = 1605, 1395, 1325, 1250, 1121, 1018, 804, 699, 660 cm^{-1}. MALDI (m/z) [M]$^+$ calculated for $C_{88}H_{84}{}^{11}B_4O_{12}$, 1376.6330, found 1376.6329. ^{1}H NMR (CD_3COCD_3, 300 MHz): δ = 8.99 (s, 4 H), 8.48 (s, 4 H), 8.28 (d, J = 4.2 Hz, 4 H), 8.04–8.03 (m, 4 H), 7.90–7.83 (m, 12 H), 6.97 (d, J = 4.1 Hz, 4 H), 4.27 (t, J = 6.6 Hz, 8 H), 2.05–1.93 (m, 8 H), 1.72–1.58 (m, 8 H), 1.51–1.38 (m, 16 H), 0.96 (t, J = 6.6 Hz, 12 H) ppm.

Assembly 8 (isolated using Method I): Reaction Scale: **2** (21.0 mg, 0.033 mmol), yield 23.4 mg (97%). The product was isolated as a black solid, m.p. > 200 °C. IR (powder, ATR): $\tilde{\nu}$ = 1699, 1607, 1489, 1396, 1325, 1234, 1066, 1017, 805, 698, 659, 576 cm^{-1}.

Assembly 9 (isolated using Method I): Reaction Scale: **3** (32.1 mg, 0.052 mmol), yield 26.5 mg (72%). The product was isolated as a grey solid that was sparingly soluble in acetone, m.p. > 200 °C. IR (powder, ATR): $\tilde{\nu}$ = 1601, 1476, 1393, 1316, 1230, 1050, 1018, 810, 659 cm^{-1}. MALDI (m/z) [M]$^+$ calculated for $C_{84}H_{76}{}^{11}B_4O_{20}$, 1448.5297, found 1448.5331. ^{1}H NMR (CD_3COCD_3, 300 MHz): δ = 8.97 (br. s, 4 H), 8.67 (br. s, 4 H), 8.42 (d, J = 8.7 Hz, 4 H), 7.92 (d, J = 8.4 Hz, 4 H), 7.84 (s, 8 H), 7.38 (d, J = 8.6 Hz, 4 H), 6.97 (d, J = 7.8 Hz, 4 H), 4.50–4.39 (m, 8 H), 3.95–3.82 (m, 8 H), 3.78–3.62 (m, 8 H), 3.62–3.51 (m, 8 H), 3.35 (br. s, 12 H) ppm.

Assembly 10 (isolated using Method I): Reaction Scale: **4** (17.9 mg, 0.026 mmol), yield 17.9 mg (82%). The product was isolated as an grey solid, m.p. > 200 °C. IR (powder, ATR): $\tilde{\nu}$ = 1604, 1477, 1396, 1319, 1234, 1060, 997, 813, 660 cm^{-1}.

Assembly 11 (isolated using Method II): Reaction scale: **5** (12.9 mg, 0.0107 mmol), yield orange solid **11** (13.9 mg, 99%). Decomposes at 199 °C. IR (powder, ATR): $\tilde{\nu}$ = 1591, 1378, 1332, 1290, 1225, 1110, 1063, 1039, 1000, 638 cm^{-1}. ^{1}H NMR ($CDCl_3$, 300 MHz): δ = 8.65 (s, 4 H), 8.28–8.12 (m, 4 H), 8.23 (s, 8 H), 7.83–7.70 (m, 8 H), 7.36–7.30 (m, 8 H), 6.72 (s, 8 H), 5.22 (s, 8 H), 3.98–3.88 (m, 24 H), 1.81–1.72 (m, 24 H), 1.55–1.43 (m, 24 H), 1.40–1.23 (m, 48 H), 0.91 (t, J = 5.0 Hz, 36 H) ppm.

Assembly 12 (isolated using Method II): Reaction scale: **6** (15.7 mg, 0.0125 mmol) yield orange solid **12** (13.9 mg, 82%). Decomposes at 185 °C. IR (powder, ATR): $\tilde{\nu}$ = 1592, 1435, 1353, 1316, 1222, 1110, 1078, 1050, 1018, 820 cm^{-1}. ^{1}H NMR ($CDCl_3$, 300 MHz): δ = 8.51 (s, 4 H), 8.06 (d, J = 20 Hz, 4 H), 7.96 (s, 8 H), 7.63–7.59 (m, 8 H), 7.20–7.15 (m, 8 H), 6.56 (s, 8 H), 4.80 (s, 8 H), 3.93 (t, J = 6.6 Hz, 8 H), 3.86 (t, J = 6.2 Hz, 16 H), 1.81–1.72 (m, 24 H), 1.52–1.42 (m, 24 H), 1.40–1.29 (m, 48 H), 0.93 (t, J = 6.6 Hz, 36 H) ppm.

Acknowledgments

This research was supported by the Wesleyan University. The authors also thank the University of California, Riverside, Mass Spectrometry Facility for mass spectrometric analysis.

[1] For reviews of dynamic covalent assembly, see: a) S. J. Rowan, S. J. Cantrill, G. R. L. Cousins, J. K. M. Sanders, J. F. Stoddart, *Angew. Chem. Int. Ed.* **2002**, *41*, 898–952; *Angew. Chem.* **2002**, *114*, 938–993; b) P. T. Corbett, J. Leclaire, L. Vial, K. R. West, J.-L. Wietor, J. M. K. Sanders, S. Otto, *Chem. Rev.* **2006**, *106*, 3652–3711; c) Y. Jin, C. Yu, R. J. Denman, W. Zhang, *Chem. Soc. Rev.* **2012**, *42*, 6634–6654; d) Y. Jin, Q. Wang, P. Taynton, W. Zhang, *Acc. Chem. Res.* **2014**, *47*, 1575–1586.

[2] For recent reviews of MOFs, see: a) M. Eddaoudi, D. B. Moler, H. L. Li, B. Chen, T. M. Reineke, M. O'Keeffe, O. M. Yaghi,

Acc. Chem. Res. **2001**, *34*, 319–330; b) J. Y. Lee, O. K. Farha, J. Roberts, K. A. Scheidt, S. T. Nguyen, J. T. Hupp, *Chem. Soc. Rev.* **2009**, *38*, 1450–1459; c) H. Furukawa, K. E. Cordova, M. O'Keeffe, O. M. Yaghi, *Science* **2013**, *341*, 974–986; as well as the **2012** issue of *Chem. Rev.* devoted to MOFs: d) Furukawa, K. E. Cordova, M. O'Keeffe, O. M. Yaghi, *Chem. Rev.* **2012**, *112*, 673–1268.

[3] The term "Metal-Organic Framework" was introduced by Yaghi in 1995, see: a) O. M. Yaghi, H. Li, *J. Am. Chem. Soc.* **1995**, *117*, 10401–10402; however structures resembling MOFs had been prepared prior to the introduction of the term, see: b) B. F. Hosking, R. Robson, *J. Am. Chem. Soc.* **1990**, *112*, 1546–1554; c) S. R. Batten, R. Robson, *Angew. Chem. Int. Ed.* **1998**, *37*, 1460–1494; *Angew. Chem.* **1998**, *110*, 1558–1595, and references cited therein.

[4] For recent reviews of COFs, see: a) X. Feng, X. Ding, D. Jaing, *Chem. Soc. Rev.* **2012**, *41*, 6010–6022; b) J. W. Colson, W. R. Dichtel, *Nat. Chem.* **2013**, *5*, 453–465; c) S.-Y. Ding, W. Wang, *Chem. Soc. Rev.* **2013**, *42*, 548–568; d) Z. Xiang, D. Cao, *J. Mater. Chem. A* **2013**, *1*, 2691–2718.

[5] A. P. Côté, A. I. Benin, N. W. Ockwig, M. O'Keeffe, A. J. Matzger, O. M. Yaghi, *Science* **2005**, *310*, 1166–1170.

[6] a) E. L. Spitler, B. T. Koo, J. L. Novotney, J. W. Colson, F. J. Uribe-Romo, G. D. Gutierrez, P. Clancy, W. R. Dichtel, *J. Am. Chem. Soc.* **2011**, *133*, 19416–19421; b) E. L. Spitler, J. W. Colson, F. J. Uribe-Romo, A. R. Woll, M. R. Giovino, A. Saldivar, W. R. Dichtel, *Angew. Chem. Int. Ed.* **2012**, *51*, 2623–2627; *Angew. Chem.* **2012**, *124*, 2677–2681.

[7] a) S. Wan, F. Gándara, A. Asano, H. Furukawa, A. Saeki, S. K. Dey, L. Liao, M. W. Ambrogio, Y. Y. Botros, X. Duan, S. Seki, J. F. Stoddart, O. M. Yaghi, *Chem. Mater.* **2011**, *23*, 4094–4097; b) X. Ding, J. Guo, X. Feng, Y. Honshihito, J. Guo, S. Seki, P. Maitarad, A. Saeki, S. Nagase, D. Jiang, *Angew. Chem. Int. Ed.* **2011**, *50*, 1289–1293; *Angew. Chem.* **2011**, *123*, 1325–1329; c) X. Feng, L. Chen, Y. Honsho, O. Saengsawang, L.-L. Liu, L. Wang, A. Saeki, S. Irle, S. Seki, Y. Gond, D. Jiang, *Adv. Mater.* **2012**, *24*, 3026–3031; d) M. Dogru, M. Handloser, F. Auras, T. Kunz, D. Medina, A. Hartschuh, P. Knochel, T. Bein, *Angew. Chem. Int. Ed.* **2013**, *52*, 2920–2924; *Angew. Chem.* **2013**, *125*, 2992–2996.

[8] X. Feng, L. L. Lui, Y. Honsho, A. Saeki, S. Seki, S. Irle, Y. P. Dong, A. Nagai, D. L. Jaing, *Angew. Chem. Int. Ed.* **2012**, *51*, 2618–2622; *Angew. Chem.* **2012**, *124*, 2672–2676.

[9] a) S.-Y. Ding, J. Gao, Q. Wang, Y. Zhang, W.-G. Song, C.-Y. Su, W. Wang, *J. Am. Chem. Soc.* **2011**, *133*, 19816–19822; b) Y. Matsushima, R. Nishiyabu, N. Takanashi, M. Haruta, H. Kimura, Y. Kubo, *J. Mater. Chem.* **2012**, *22*, 24124–24131.

[10] a) S. S. Han, H. Furukawa, O. M. Yaghi, W. A. Goddard, *J. Am. Chem. Soc.* **2008**, *130*, 11580–11581; b) D. P. Cao, J. H. Lan, W. C. Wang, B. Smit, *Angew. Chem. Int. Ed.* **2009**, *48*, 4730–4733; *Angew. Chem.* **2009**, *121*, 4824–4827; c) H. Furukawa, O. M. Yaghi, *J. Am. Chem. Soc.* **2009**, *131*, 8875–8883.

[11] O. M. Yaghi, M. O' Keefe, N. Ockwig, H. Chae, M. Eddaoudi, J. Kim, *Nature* **2003**, *423*, 705–714.

[12] a) N. Fujita, S. Shinkai, T. D. James, *Chem. Asian J.* **2008**, *3*, 1076–1091; b) K. Severin, *Dalton Trans.* **2009**, 5254–5264; c) R. Nishiyabu, Y. Kubo, T. D. James, J. S. Fossey, *Chem. Commun.* **2011**, *47*, 1124–1150; d) S. D. Bull, M. G. Davidson, J. M. van den Elsen, J. S. Fossey, A. T. A. Jenkins, Y.-B. Jiang, Y. Kubo, F. Marken, K. Sakurai, J. Zhao, T. D. James, *Acc. Chem. Res.* **2013**, *46*, 312–326.

[13] a) R. W. Tilford, W. R. Gemmill, H.-G. zur Loye, J. J. Lavigne, *Chem. Mater.* **2006**, *18*, 5296–5301; b) A. P. Côté, H. M. El-Kaderi, H. Furukawa, J. R. Hunt, O. M. Yaghi, *J. Am. Chem. Soc.* **2007**, *129*, 12914–12915; c) H. M. El-Kaderi, J. R. Hunt, J. L. Mendoza-Cortés, A. P. Côté, R. E. Taylor, M. O'Keeffe, O. M. Yaghi, *Science* **2007**, *316*, 268–272; d) R. W. Tilford, S. J. Magavero, P. J. Pellechia, J. J. Lavigne, *Adv. Mater.* **2008**, *20*, 2741–2746; e) M. Dogru, A. Sonnauer, A. Gavryushin, P. Knochel, T. Bein, *Chem. Commun.* **2011**, *47*, 1707–1709; f) J. F. Dienstmaier, D. D. Medina, M. Dogru, P. Knochel, T. Bein, W. M. Heckl, M. Lackinger, *ACS Nano* **2012**, *6*, 7324–7242; g) J.-T. Yu, Z. Chen, J. Sun, Z.-T. Huang, Q.-Y. Zheng, *J. Mater. Chem.* **2012**, *22*, 5369–5373; h) X. Feng, Y. Dong, D. Jiang, *CrystEngComm* **2013**, *15*, 1508–1511.

[14] K. Kataoka, T. D. James, Y. Kubo, *J. Am. Chem. Soc.* **2007**, *129*, 15126–15127.

[15] a) N. Christinat, R. Scopelliti, K. Severin, *Angew. Chem. Int. Ed.* **2008**, *120*, 1874–1878; *Angew. Chem.* **2008**, *47*, 1848–1852; b) B. Icli, N. Christinat, J. Tönnemann, C. Schüttler, R. Scopelliti, K. Severin, *J. Am. Chem. Soc.* **2009**, *131*, 3154–3155.

[16] a) N. Nishimura, K. Kobayashi, *Angew. Chem. Int. Ed.* **2008**, *47*, 6255–6258; *Angew. Chem.* **2008**, *120*, 6251–6254; b) N. Nishimura, K. Yoza, K. Kobayashi, *J. Am. Chem. Soc.* **2010**, *132*, 777–790; c) N. Nishimura, K. Kobayashi, *J. Org. Chem.* **2010**, *75*, 6079–6085; d) M. Mitsui, K. Higashi, R. Takahashi, Y. Hirumi, K. Kobayashi, *Photochem. Photobiol. Sci.* **2014**, *13*, 1130–1136.

[17] a) N. Iwasawa, H. Takahagi, *J. Am. Chem. Soc.* **2007**, *129*, 7754–7755; b) H. Takahagi, S. Fujibe, N. Iwasawa, *Chem. Eur. J.* **2009**, *15*, 13327–13330; c) S. Ito, k. Ono, N. Iwasawa, *J. Am. Chem. Soc.* **2012**, *134*, 13962–13965; d) S. Ito, H. Takata, K. Ono, N. Iwasawa, *Angew. Chem. Int. Ed.* **2013**, *52*, 11045–11048; *Angew. Chem.* **2013**, *125*, 11251–11254.

[18] a) G. Zhang, O. Presly, F. White, I. M. Oppel, M. Mastalerz, *Angew. Chem. Int. Ed.* **2014**, *126*, 1542–1546; *Angew. Chem.* **2014**, *126*, 1516–1520; b) G. Zhang, O. Presly, F. White, I. Oppel, M. Mastalerz, *Angew. Chem. Int. Ed.* **2014**, *53*, 5126–5130; *Angew. Chem.* **2014**, *126*, 5226–5230.

[19] T.-H. Chen, W. Kaveevivitchai, N. Bui, O. S. Miljanić, *Chem. Commun.* **2012**, *48*, 2855–2857.

[20] For representative examples of the use of B–N coordination in self-assembled boronate ester materials, see: a) H. Höpfl, *J. Organomet. Chem.* **1999**, *581*, 129–149; b) N. Christinat, R. Scopelliti, K. Severin, *Chem. Commun.* **2004**, 1158–1159; c) V. Barba, I. Betanzos, *J. Organomet. Chem.* **2007**, *692*, 4903–4908; d) N. Christinat, R. Scopelliti, K. Severin, *J. Org. Chem.* **2007**, *72*, 2192–2200; e) N. Christinat, R. Scopelliti, K. Severin, *Chem. Commun.* **2008**, 3660–3662; f) M. Hutin, G. Bernardinelli, J. R. Nitschke, *Chem. Eur. J.* **2008**, *14*, 4585–4593.

[21] For recent reviews of shape-persistent polygons and polyhedra, see: a) S. Höger, *Chem. Eur. J.* **2004**, *10*, 1320–1329; b) W. Zhang, J. S. Moore, *Angew. Chem. Int. Ed.* **2006**, *45*, 4416–4439; *Angew. Chem.* **2006**, *118*, 4524–4548; c) G. Zhang, M. Mastalerz, *Chem. Soc. Rev.* **2014**, *43*, 1943–1947.

[22] L. A. Tatum, C. J. Johnson, A. A. P. Fernando, B. C. Ruch, K. K. Barakoti, M. A. Alpuche-Aviles, B. T. King, *Chem. Sci.* **2012**, *3*, 3261–3264.

[23] T. Wöhrle, A. Baro, S. Laschat, *Materials* **2014**, *7*, 4045–4056.

[24] Several methods have been reported for the preparation of COFs on solid surfaces, including ultrahigh vacuum deposition, see: a) N. A. A. Zwaneveld, R. Pawlak, M. Abel, D. Catalin, D. Gigmes, D. Bertin, L. Porte, *J. Am. Chem. Soc.* **2008**, *130*, 6678–6679; b) S. Clair, M. Able, L. Porte, *Chem. Commun.* **2014**, *50*, 9627–9635; for Ullmann coupling, see: c) T. Faury, S. Clair, M. Abel, F. Dumur, D. Gigmes, L. Porte, *J. Phys. Chem. C* **2012**, *116*, 4819–4823; for drop-casting followed by thermal dehydration, see: d) J. F. Dienstmaier, A. M. Gigler, A. J. Goetz, P. Knochel, T. Bein, A. Lyapin, S. Reichlmaier, W. M. Heckl, M. Lackinger, *ACS Nano* **2011**, *5*, 9737–9745; e) C.-Z. Guan, D. Wang, L.-J. Wan, *Chem. Commun.* **2012**, *48*, 2943–2945; f) J. F. Dienstmaier, D. D. Medina, M. Dogru, P. Knochel, T. Bein, M. Heckl, M. Lackinger, *ACS Nano* **2012**, *6*, 7234–7242; and under solvothermal conditions: g) J. W. Colson, A. R. Woll, A. Mukherjee, M. P. Levendorf, E. L. Spitler, V. B. Shields, M. G. Spencer, J. Park, W. R. Dichtel, *Science* **2011**, *332*, 228–231; and ref.[6b].

[25] See, for example: a) W. Niu, B. Rambo, M. D. Smith, J. J. Lavigne, *Chem. Commun.* **2005**, 5166–5168; b) W. Niu, M. D. Smith, J. J. Lavigne, *Cryst. Growth Des.* **2006**, *6*, 1274–1277.

[26] Three distinct covalent nitroso polymer networks have been solved by single-crystal X-ray diffraction, see: D. Beaudoin, T. Maris, J. D. Wuest, *Nat. Chem.* **2013**, *5*, 830–834.
[27] Single-crystals of an imine-based framework have been solved using 3D electron diffraction analysis applying the method of rotation electron diffraction (RED) for data collection, see: Y.-B. Zhang, J. Su, H. Furukawa, Y. Yun, F. Gándara, A. Duong, X. Zou, O. M. Yaghi, *J. Am. Chem. Soc.* **2013**, *135*, 16336–16339.
[28] B. J. Smith, W. R. Dichtel, *J. Am. Chem. Soc.* **2014**, *136*, 8783–8789.
[29] M. K. Smith, N. P. Powers-Riggs, B. H. Northrop, *Chem. Commun.* **2013**, *49*, 6167–6169.
[30] L. M. Lanni, R. W. Tilford, M. Bharathy, J. J. Lavigne, *J. Am. Chem. Soc.* **2011**, *133*, 13975–13983.
[31] a) K. Tanabe, T. Yasuda, M. Yoshio, T. Kato, *Org. Lett.* **2007**, *9*, 4271–4274; b) R. van de Coevering, P. Bruijnincx, C. Walree, J. Gebbink, G. van Koten, *Eur. J. Org. Chem.* **2007**, *18*, 2931–2939; c) P. Dechambenoit, S. Ferlay, B. Donnio, D. Guillon, M. W. Hosseini, *Chem. Commun.* **2011**, *47*, 734–736.
[32] M. K. Smith, B. H. Northrop, *Chem. Mater.* **2014**, *26*, 3781–3795.
[33] Recent research by Dichtel et al. has suggested that the formation of 2D COFs may proceed by a templated polymerization mechanism largely driven by intermolecular interactions wherein growing COF oligomers template the addition and reaction of additional monomers, see ref.[28].
[34] V. Percec, M. Mihai, Y. Tsuda, B. M. Rosen, S. Uchida, M. R. Imam, G. Ungar, P. A. Heiney, *Chem. Eur. J.* **2009**, *15*, 8994–9004.
[35] B. Boden, J. Hui, M. MacLachlan, *J. Org. Chem.* **2008**, *73*, 8069–8072.

Received: February 5, 2015
Published Online: ■

EurJOC European Journal of Organic Chemistry

Getting in and out of the library: Six phenanthrene-based bis(catechol) derivatives are reported and their ability to undergo dynamic covalent self-assembly with benzenediboronic acid is investigated. The influence of different solubilizing groups at the 9- and 10-positions of phenanthrene, the effects of greater or lesser π-surface area, and the influence of hydrophobic and protic solvents on the efficacy of self-assembly are each investigated.

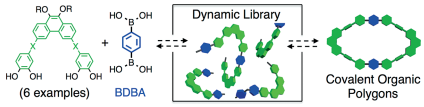

Keywords: Self-assembly / Macrocycles / Borates

